Supplemental Material

Supplementary Materials and Methods

Measurement of Apoptosis. As measure of cell viability, apoptosis was measured in cells after 48 hours in culture for one visit from a subset of six volunteers (3 males, 3 females). Cells were treated with $HgCl_2$ concentrations up to 200 nM in the presence or absence of 50 ng/ml LPS. After harvesting by gentle agitation, cells were stained according to manufacturer's recommended protocol for the AnnexinV-FITC Apoptosis Detection Kit (BD Pharmingen, San Jose, CA). Briefly, cells were washed twice with cold PBS and resuspended in binding buffer. Cells were incubated on ice for fifteen minutes in the dark with FITC-AnnexinV and Propidium Iodide (PI). Excess buffer (400μl) was added to each tube, and cells were analyzed by flow cytometry within one hour using a BD FACSCalibur instrument.

Measurement of Cell Population Markers. Cell subsets and activation markers were also measured by flow cytometry at the end of each exposure period for the culture conditions described above (up to 200 nM $HgCl_2$). The following mouse anti-human monoclonal antibodies (mAbs) were obtained from BD Pharmingen (San Jose, CA): AlexaFluor488-conjugated anti-CD11b, PE-conjugated anti-CD19, PE-Cy7-conjugated anti-CD3, PE-conjugated CD4, FITC-conjugated anti-CD8. After harvesting by gentle agitation, cells were incubated on ice in the dark for 20 minutes with the selected fluor-conjugated mAbs. Cells were washed with cold 1% Bovine Serum Albumin (Fisher Scientific) in PBS, and centrifuged at 4°C and 1100xg for seven

minutes. Cells were resuspended in 250 μL of cold 1% para-formaldehyde in PBS and analyzed by flow cytometry using a BD FACS LSR II instrument.

Analysis of Flow Cytometry Data. Flow cytometry data were analyzed using FlowJo Software (Tree Star, Inc., Ashland, OR). After plotting forward scatter versus side scatter, cells were gated to include lymphocyte, monocyte, and macrophage populations according to size and complexity of the cells. Non-stained and singly-stained controls were used for compensation of the instrument and to appropriately set gates which determined the threshold for each signal.

We used univariate linear regression on the concentration-response curves to test for a trend as a result of $HgCl_2$ treatment on cell viability or population markers. $P_{[Hg]}$ is defined as the p-value for the slope of the concentration-response curve for each endpoint, which tests the null hypothesis that the slope of the concentration-response curve is equal to zero. Data from LPS-treated cells was analyzed separately from the data gathered for cells treated with $HgCl_2$ only. Linear regression analyses were conducted using STATA10 software (STATAcorp LP, version 10IC).

Supplemental Results

Low concentrations of $HgCl_2$ do not induce cell death or changes in cell populations. To ensure that any differences observed between cells at different mercury concentrations were not due to the cytotoxic effects of mercury, we first examined cell viability under the treatment conditions used. No changes were observed in the percent of apoptosing cells (AnnexinV+PI-), dead or necrosing cells (AnnexinV+PI+), or living cells (AnnexinV-PI-) in response to treatment with up to 200 nM $HgCl_2$, both in the presence and absence of LPS (Supplemental Material,

Figure 2). Thus, the results eliminate a nonspecific cytotoxic effect of Hg on any changes in cytokine concentration measured in this study.

There were no changes in cell subpopulations (CD3-CD19+ B cells, CD3+CD4+ T cells, CD3+CD8+ T cells, CD11b+ monocytes and macrophages) within the PBMC cultures as a result of $HgCl_2$ treatment (Supplemental Material, Table 1).

Model Selection. A visual inspection of all Phase 1 concentration-response curves for TNF-α (Supplemental Material, Figure 3A-B) indicates that the cytokine response to LPS alone is highly variable (the intercept of the concentration-response curve in this case). When plotted on the natural scale (Supplemental Material, Figure 3C), the skewed nature of the observed intercept values is shown. Log-transformation of the data reduces the skewness of the distribution (Supplemental Material, Figure 3D). Because accurate model parameter estimation is dependent upon the assumption that continuous data such as cytokine concentrations are normally distributed, we log transformed all data before model fitting.

In Supplemental Material, Figure 3E, twenty TNF-α concentration-response curves were selected on the basis of their intercept value so that five curves from each quartile are represented. These data were plotted on the log scale to show the overall distribution of intercepts. The observed intercept value was subtracted from each of the 20 concentration-response curves, and the curves were plotted again on a shifted scale in Supplemental Material, Figure 3F, with each intercept now at the origin. The variability in the data is greatly reduced, revealing a consistent increase in TNF-α in response to $HgCl_2$ treatment at each of these 20

visits. The variation observed in the intercept of the concentration-response curves suggests that a model with a random intercept is appropriate to describe the dataset.

Because the variation observed in the cytokine response data is more a product of the variation observed in the intercept, or the baseline response to LPS, than of the variation in the slope, or response to $HgCl_2$, plotting the observed intercepts for each of the visits of each of the subjects therefore represents a substantial portion of the inter- and intra-individual variation observed in the data. The observed intercepts for each visit are plotted about the mean of the observed intercepts for each subject in Supplemental Material, Figure 4C. The model prediction for the mean subject intercept, b_{0i}, for each subject is also shown. Bayesian modeling borrows information across all levels of the model in order to estimate the parameters for each level. Observations with less variability are weighted more heavily than those with relatively larger amounts of variability. This often results in "shrinkage" of model estimates toward the overall mean, especially for subjects or visits where greater variability is observed in the cytokine response. In this case, information from the entire dataset has been used to estimate each subject-specific mean intercept b_{0i}, which are often shrunk toward the overall mean for the population, β_0=5.66. Observed mean subject intercepts for each subject are directly compared with their predicted mean subject intercept (b_{0i}) counterpart in Supplemental Material, Figure 4D.

Supplemental Material, Figure 1. *Study Design.* In Phase 1, 20 healthy, adult volunteers (10 males and 10 females) were recruited from the Johns Hopkins Medical Institution community. Volunteers were asked to donate 20 ml of blood and answer a brief questionnaire about their lifestyle and health status. These 20 subjects (i=20) were asked to repeat this process six times, for a total of six visits (j=6/subject) to the laboratory spanning a time period of at least six months. PBMCs were separated from the blood using Ficoll gradient, and cultured at a density of 10^6 cells/ml in media containing 0, 10, 100, or 200 nM $HgCl_2$, in the presence or absence of 50ng/ml LPS in addition to $HgCl_2$. All treatment groups were cultured in triplicate, as shown. Supernatants from each well were assayed for cytokine concentration (k=24/cytokine). After the completion of Phase 1, an additional 20 healthy adult volunteers were recruited for Phase 2. These volunteers were asked to donate blood and answer a questionnaire only once. Results for each cytokine tested in Phase 1 were modeled, and estimates of the model parameters were compared to estimates generated by modeling the cytokine data collected in Phase 2.

Supplemental Material, Figure 1.

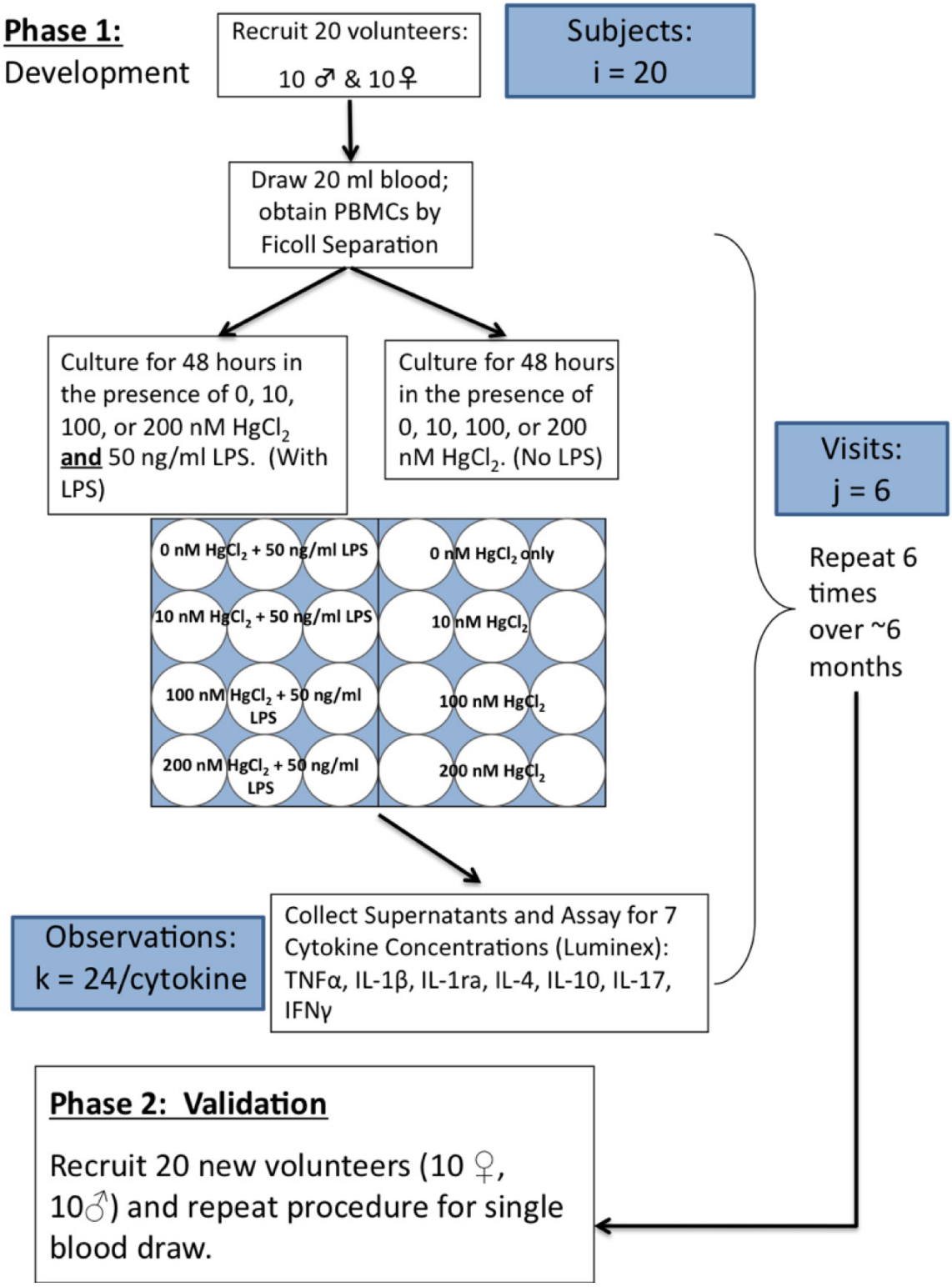

Supplemental Material, Figure 2. *Low concentrations of $HgCl_2$ do not induce cell death.* PBMCs isolated from a subset of six volunteers (3 males, 3 females) were treated with increasing concentrations of $HgCl_2$ (up to 200 nM) in the presence and absence of 50 ng/ml LPS, and stained for the apoptosis marker Annexin-V and general cell death marker PI. No changes were observed in response to $HgCl_2$ treatment up to 200nM in the percentage of apoptosing cells (% Annexin-V positive and PI negative) in cells treated with HgCl2 only (**A**) and cells treated with both $HgCl_2$ and LPS (**B**). Similarly, no changes were observed in response to $HgCl_2$ treatment up to 200nM in the percentage of dead cells (% Annexin-V positive and PI positive) in cells treated with $HgCl_2$ only (**C**) and cells treated with both $HgCl_2$ and LPS (**D**).

Supplemental Material, Figure 2.

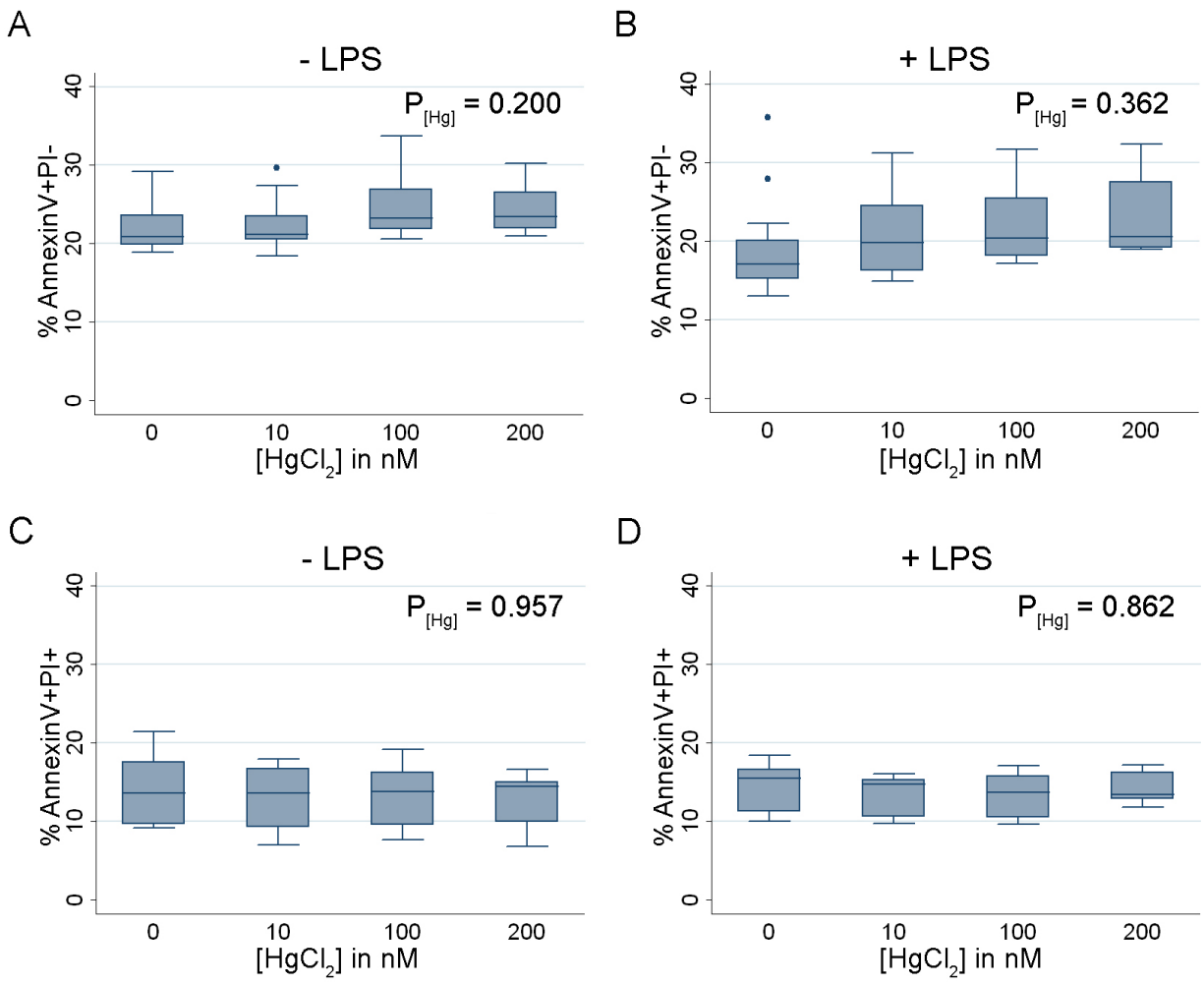

Supplemental Material, Figure 3. *TNF-α production increases in a concentration-response manner with $HgCl_2$ treatment in the presence of LPS, though subjects differ in their baseline response to LPS.* **A.** The concentration-response curves for TNF-α production in response to $HgCl_2$ (in the presence of 50 ng/ml LPS) are shown for all Phase 1 volunteers (n=20) for all visits (n=111) on their original scale. Each volunteer is plotted in a different color. **B.** The concentration-response curves described in Fig. 2A are represented after $\log_e$ transformation. **C.** The observed mean value from each visit when cells are treated with no $HgCl_2$ (0 nM $HgCl_2$) and 50 ng/ml LPS can be considered the intercept of the concentration-response curve for LPS-treated cells. These observed mean intercept values from all Phase 1 volunteers (n=20) for all visits (n=111) are represented in a histogram on their original scale, with the solid black denoting a normal curve based on the sample mean and standard deviation and the dashed red line denoting a kernel-density estimate. **D.** The observed mean intercepts from all Phase 1 volunteers (n=20) for all visits (n=111) after $\log_e$ transformation are represented in a histogram. As in Fig. 2C, the solid black denotes a normal curve based on the sample mean and standard deviation and the dashed red line denotes a kernel-density estimate. **E.** Five visits from each quartile (based on observed, log-transformed mean intercepts of the concentration-response curves from all visits) were randomly selected, and the data for ln([TNF-α]) for these visits are plotted against the concentration (in nM) of $HgCl_2$. **F.** The mean intercept value from each visit represented in E was subtracted from the concentration-response curve for each corresponding visit, and the data were plotted on a shifted scale.

Supplemental Material, Figure 3.

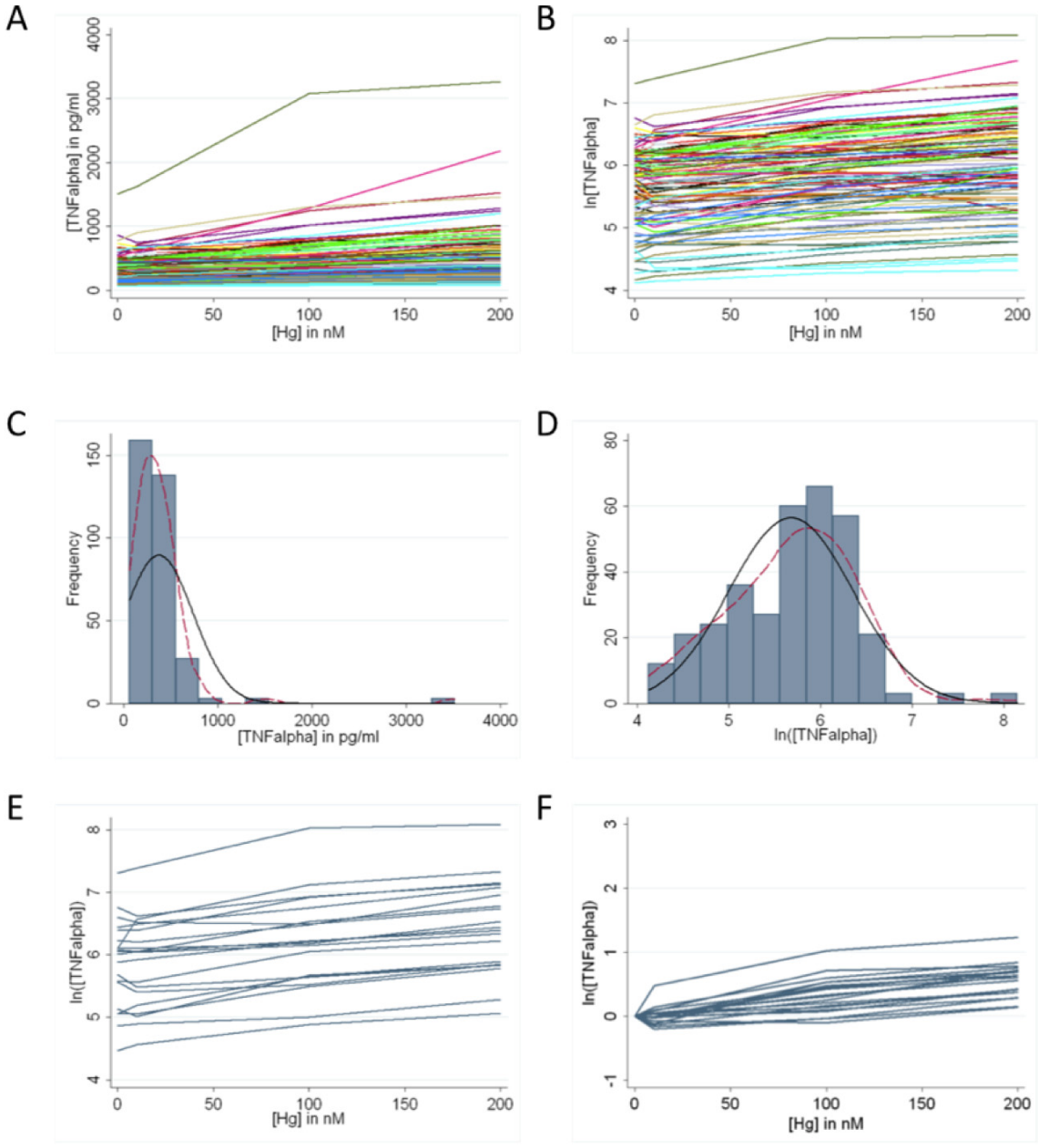

Supplemental Material, Figure 4. *Variable responses in TNF-α are shrunk toward the mean response with Bayesian modeling approach.* **A.** The observed TNF-α concentration-response curves for a single male subject with a wide range of variability in the baseline response to LPS is shown for all six visits as a solid line, and the model-predicted concentration-response curve for the corresponding visit is shown in a dashed line. Each visit is represented in a different color, along with the predicted mean subject concentration-response curve for that volunteer as a solid red line. **B.** The observed and predicted TNF-α concentration-response curves are displayed as in Fig. 3A for a female subject with relatively little variability in the baseline response to LPS. **C.** The observed intercept (or baseline response to LPS) is shown for every visit (black diamonds) plotted about the mean of the observed intercepts for that subject (red squares). The model-predicted subject mean (blue circles) for each subject are also shown. **D.** The observed subject mean intercept (red squares, as in Fig. 3C) are shown in relation to the corresponding predicted subject mean intercept (blue circles).

Supplemental Material, Figure 4.

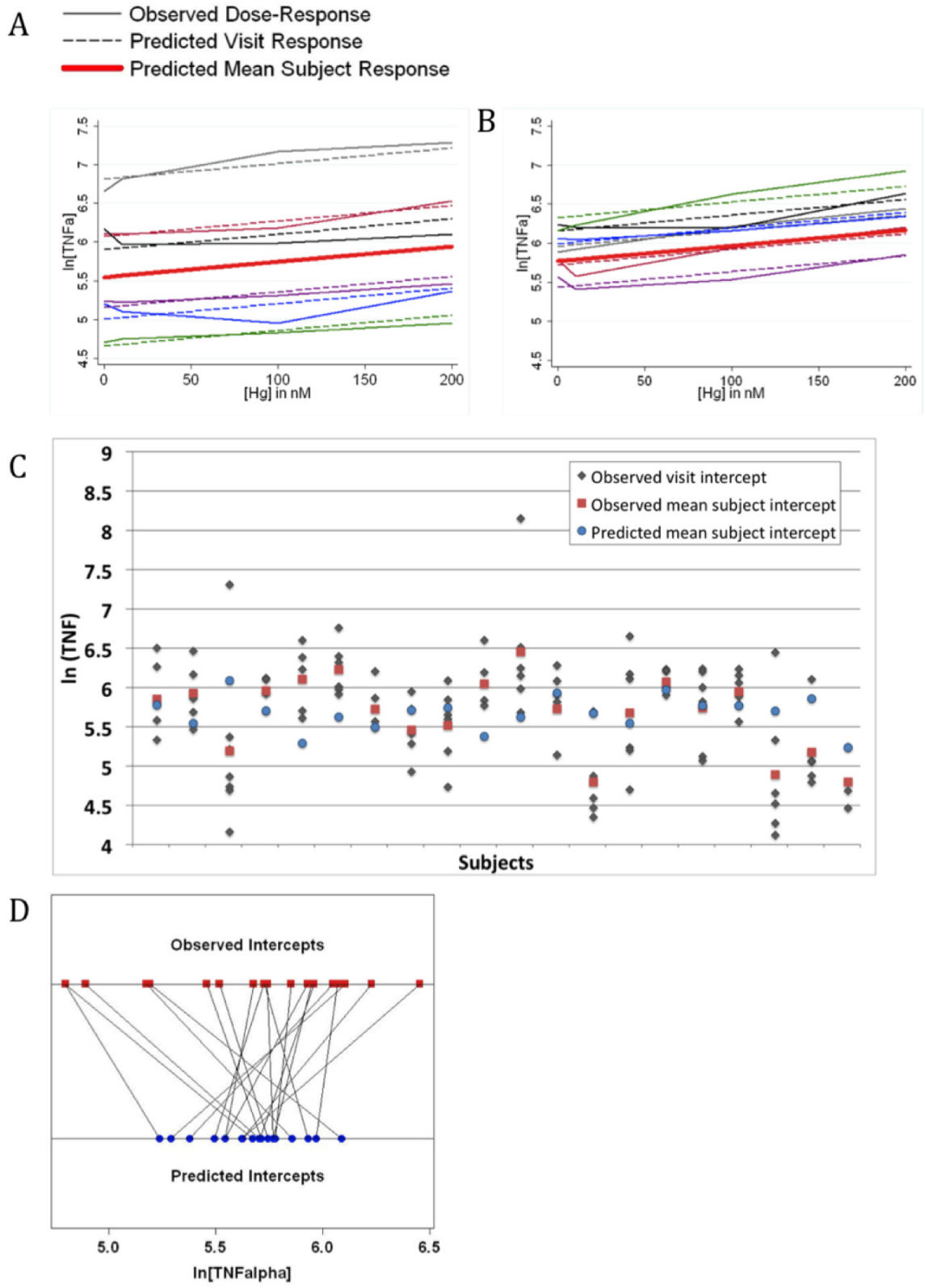

Supplemental Material, Figure 5. *$HgCl_2$ increases pro-inflammatory cytokine production and decreases anti-inflammatory cytokine production in the presence of LPS.* **A.** IL-1β production increases in a concentration-response manner with $HgCl_2$ treatment in the presence of LPS. Observed concentration-response curves from 20 subjects at a single visit (j=3) are depicted with a solid line, while the predicted concentration-response curve from Model Y is shown with a dashed line. **B.** The observed IL-1β concentration-response curves for a single female subject (i=17) at all six visits are shown in a solid line, and the model-predicted concentration-response curve for the corresponding visit is shown in a dashed line. Each visit is represented in a different color, along with the predicted mean subject concentration-response curve for that volunteer as a solid red line. **C.** IL-1Ra decreases in a concentration-response manner with $HgCl_2$ treatment in the presence of LPS. Observed and predicted concentration-response curves for IL-1Ra for 20 subjects at a single visit (j=3) are depicted as in Fig. 4A. **D.** IL-1Ra concentration-response curves for a single subject (i=17) at all six visits are depicted as in 4B. **E.** IL-10 decreases in a concentration-response manner with $HgCl_2$ treatment in the presence of LPS. Observed and predicted concentration-response curves for IL-10 for 20 subjects at a single visit (j=3) are depicted as in Fig. 4A. **F.** IL-10 concentration-response curves for a single subject (i=17) at all six visits are depicted as in 4B.

Supplemental Material, Figure 5.

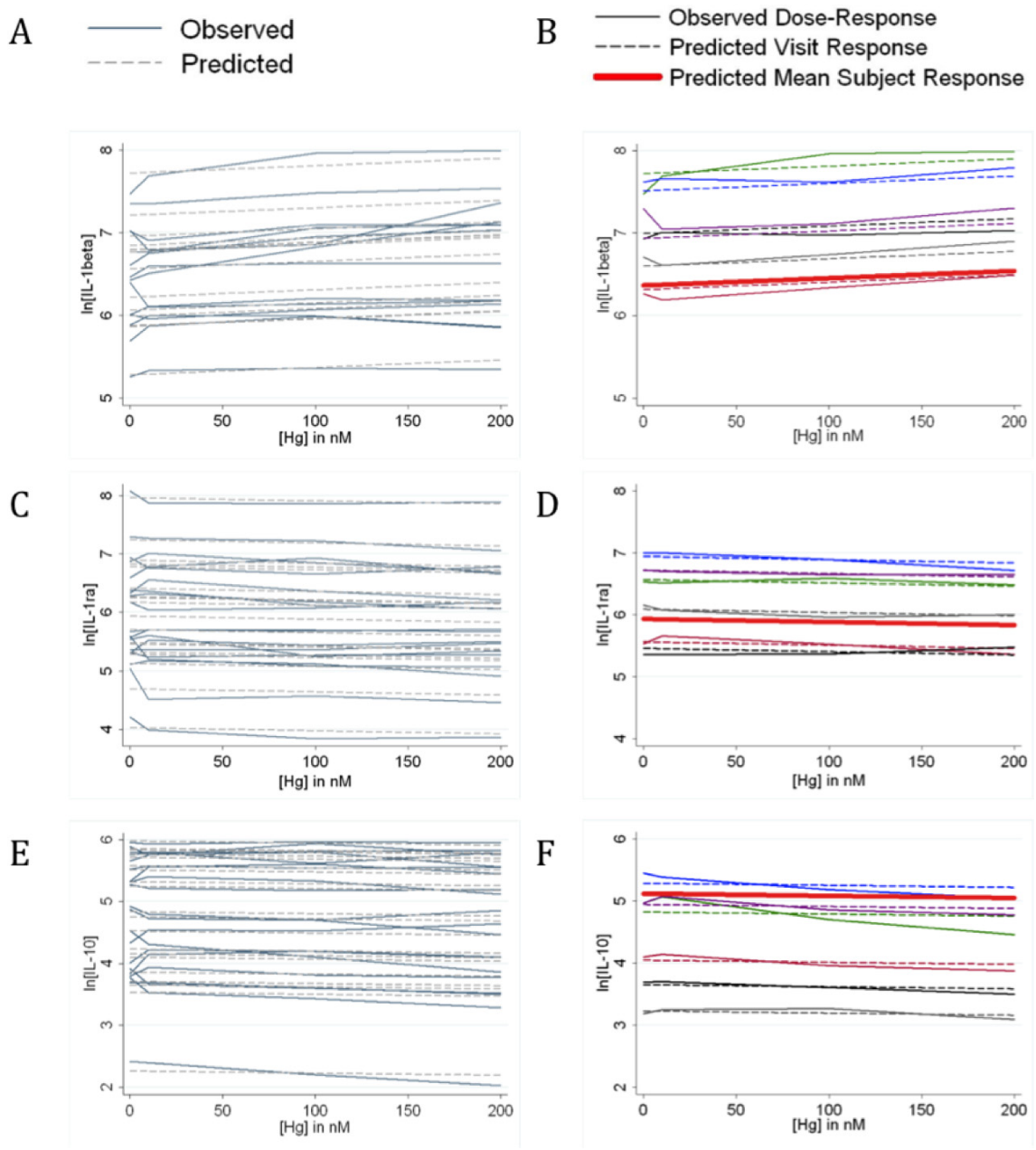

Supplemental Material, Figure 6. *$HgCl_2$ also increases IL-4, IL-17, and IFN-γ production in the presence of LPS.* **A.** IL-4 production increases in a concentration-response manner with $HgCl_2$ treatment in the presence of LPS. Observed concentration-response curves from 20 subjects at a single visit (j=3) are depicted with a solid line, while the predicted concentration-response curve from Model Y is shown with a dashed line. **B.** IL-17 production increases in a concentration-response manner with $HgCl_2$ treatment in the presence of LPS. Observed and predicted concentration-response curves for IL-17 for 20 subjects at a single visit (j=3) are depicted as in Supp. Fig. 5A. **C.** IFN-γ production increases in a concentration-response manner with $HgCl_2$ treatment in the presence of LPS. Observed and predicted concentration-response curves for IFN-γ for 20 subjects at a single visit (j=3) are depicted as in Supp. Fig. 5A.

Supplemental Material, Figure 6.

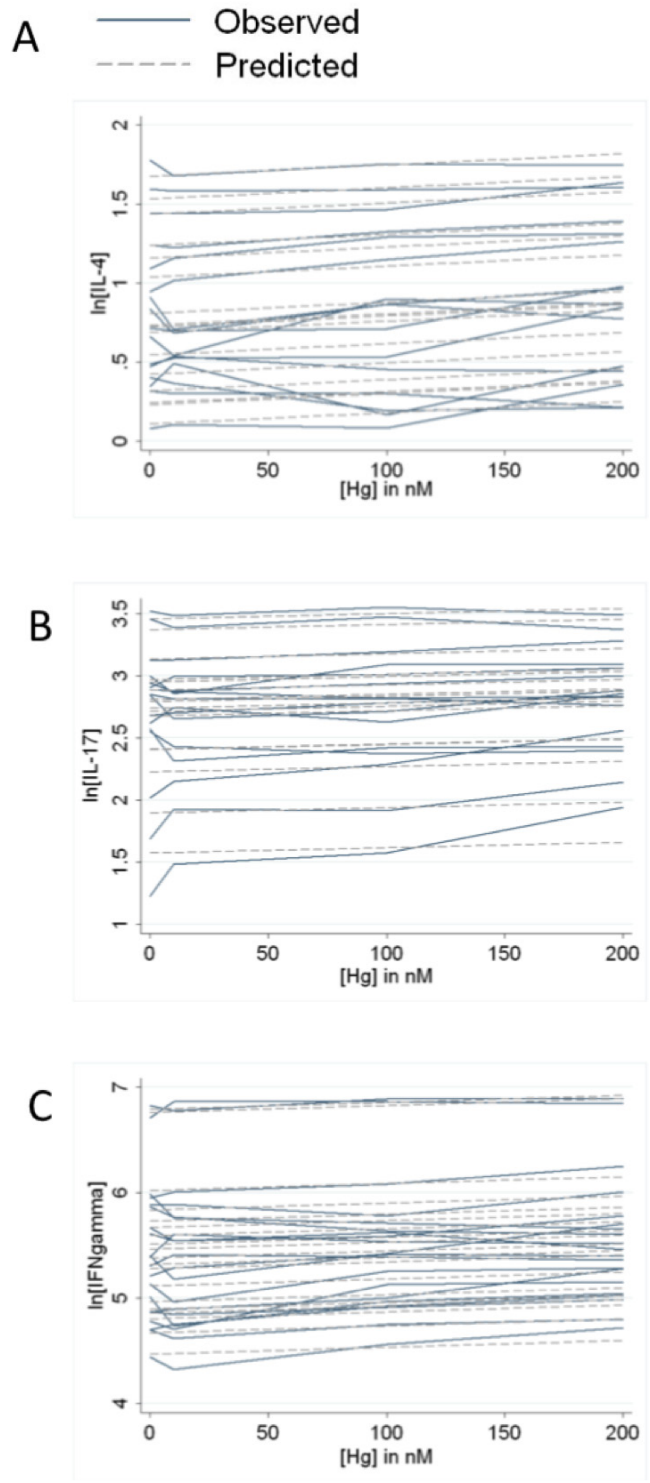

Supplemental Material, Figure 7. *Power simulation for precise estimation of* σ^2_A. Larger datasets were simulated based on the effect size and variance observed in the cytokine data collected. The posterior distribution of σ^2_A was estimated for each simulated dataset, and the T statistic for σ^2_A (mean/SE) was calculated. The estimated T statistics are presented assuming that the number of visits remained at six per volunteer (solid line, j = 6) or that the number of visits was reduced to three per volunteer (dashed line, j = 3). We assume that adequate power will be attained when T = 2.

Supplemental Material, Figure 7.

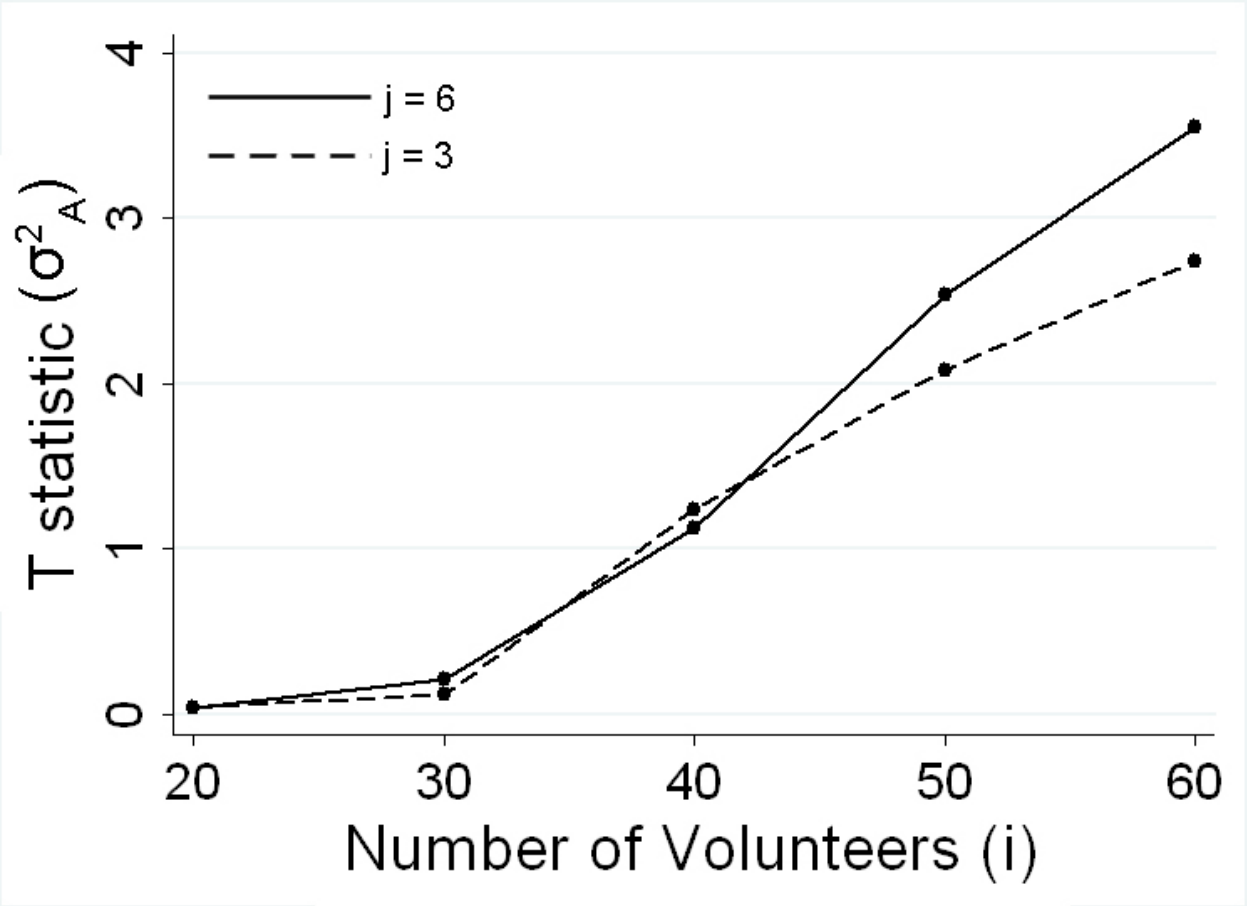

Supplemental Material, Table 1

Cell population	LPS	0 nM $HgCl_2$	200 nM $HgCl_2$	$P_{[Hg]}$[a]
B cells				
CD3-CD19+	+	9.5 (3.7 – 17.7)[b]	9.1 (3.9 – 19.3)	0.331
	-	10.3 (5.4 – 16.0)	9.0 (5.7 – 15.7)	0.641
T cells				
CD3+CD4+	+	26.0 (19.5 – 30.3)	25.9 (18.1 – 30.5)	0.904
	-	27.1 (24.5 – 29.4)	27.1 (23.9 – 30.4)	0.702
CD3+CD8+	+	12.6 (2.6 – 20.9)	12.8 (2.5 – 21.9)	0.873
	-	10.6 (3.5 – 15.5)	10.5 (2.5 – 16.3)	0.669
Monocytes and Macrophages				
CD11b+	+	14.2 (7.9 – 19.7)	14.0 (8.3 – 17.6)	0.764
	-	15.9 (10.4 – 20.9)	16.3 (9.9 – 19.9)	0.707

a: $P_{[Hg]}$ represents the p-value for the trend in $HgCl_2$ effect in the concentration-response curve for data from six volunteers (three males and three females) after PBMCs were cultured for 48 hours with 0, 10, 100, or 200 nM $HgCl_2$ and in the presence or absence of LPS, as noted.
b: The mean (minimum – maximum) is shown for each group.